

NEUTRON RESONANCES IN BROMINE

D. ZELIGER, N. ILIESCU, KIM HI SAN, D. LONGO, L. B. PIKEL'NER, and É. I. SHARAPOV

Joint Institute for Nuclear Research

Submitted to JETP editor March 1, 1963

J. Exptl. Theoret. Phys. (U.S.S.R.) **45**, 1294-1303 (November, 1963)

Bromine neutron resonance in the energy range up to 400 eV is investigated by the time of flight method with detectors for recording capture and scattering. The parameters of 15 resonances are obtained. The level spins are determined for 9 resonances. For 5 levels $J = 1$ and for four $J = 2$.

THE purpose of research on neutron resonances of nuclei is to obtain information on the parameters of the levels in the region of the neutron binding energy. This includes the neutron and radiation widths Γ_n and Γ_γ , and the level spin J .

The present work is devoted to an investigation of the radiative capture and scattering of neutrons by bromine nuclei, and is aimed at making the level parameters more precise and obtaining the spins, which hitherto have not been determined for bromine.

The bromine neutron resonance parameters were investigated by the transmission method in the work of Leblanc et al.^[1] The values of $g\Gamma_n$ and Γ were obtained for nine resonances at neutron energies up to 317 eV [$g = (2J+1)/2(2I+1)$, where I is the spin of the nucleus in the ground state]. The radiation widths were determined by Rosen et al.^[2], but no values were obtained for the level spins.

In the present investigation, the cross sections for radiative capture and neutron scattering were measured by the time of flight method using the pulsed fast reactor (IBR) of the Joint Institute for Nuclear Research^[3] as a neutron source.

The flight base was 750 m for measurement with the $n\gamma$ detector and 500 m for measurement with the scattered-neutron detector. This ensured a resolution of 0.05 and 0.08 $\mu\text{sec}/\text{m}$, respectively. The time spectrum was registered by a 1024-channel time analyzer^[4] with an 8- μsec channel width.

The radiative capture was measured with the aid of a liquid scintillation $n\gamma$ detector^[5]. The neutron scattering was investigated with a scintillation detector based on $\text{ZnS}(\text{Ag}) + \text{B}$ (light-sensitive compound T-1)^[6].

RADIATIVE NEUTRON CAPTURE

Consider a sample D located inside a detector perpendicular to the incident neutron beam. We denote the thickness of the sample by n_D (nuclei/ cm^2). The number of detector counts connected with the registration of the radiative neutron capture per time channel can be written in the form

$$N(D) = \int \Pi(E') \Delta E' [1 - \exp(-n_D \sigma_t)] \times \frac{\sigma_\gamma}{\sigma_t} \epsilon_\gamma R(E - E') dE', \quad (1)$$

where $\Pi(E)$ —number of neutrons in a unit energy interval (corresponding to the time of flight t), incident on the entire area of the sample during the measurement time; $\Delta E = (2\Delta t/t)E$ —energy width of the time channel Δt ; σ_t and σ_γ —total and capture cross sections at energy E , with account of the Doppler broadening; ϵ_γ —efficiency with which the detector registers a radiative capture event; $R(E - E')$ —resolution function.

The total counting rate in all the channels containing an isolated resonance does not depend on the resolution and is equal to

$$\sum N(D) = \int \Pi(E) [1 - \exp(-n_D \sigma_t)] \frac{\sigma_\gamma}{\sigma_t} \epsilon_\gamma dE. \quad (2)$$

Expression (2) can be reduced under certain approximations to the form¹⁾

$$\sum N(D) = \Pi(E_0) \epsilon_\gamma \frac{\Gamma_\gamma}{\Gamma} \int [1 - \exp(-n_D \sigma_r)] dE, \quad (3)$$

where σ_r is the resonant term of the total cross section.

The integral in the right half of (3) is the area A_D under the dip on the transmission curve. This area is a function of the resonance parameters $g\Gamma_n$ and Γ_n , the Doppler width Δ , and the thick-

¹⁾An estimate of the precision of such an approximation is given in [14].

ness n_D of the sample. Tables of A_D are given in [7].

Expression (3) can then be written in the form

$$\Sigma N(D)/\Pi(E_0)\epsilon_\gamma = A_D\Gamma_\gamma/\Gamma = C. \quad (4)$$

To determine C it is necessary to find the product $\Pi(E_0)\epsilon_\gamma$. For the investigated bromine specimen, this product was determined from the detector count at the maximum of a strong and well resolved resonance with energy 35.9 eV. Measurements with samples of different thicknesses have shown that the count at the maximum remains constant, i.e., all the neutrons of resonant energy are absorbed in the samples. It then follows from (1) that

$$N(D) = \Pi(E_0)\Delta E\epsilon_\gamma\Gamma_\gamma/\Gamma. \quad (5)$$

Bearing in mind that the ratio Γ_γ/Γ at small values of Γ_n (see the table below) depends weakly on the absolute values of Γ_γ and Γ , we can determine $\Pi(E_0)\epsilon_\gamma$ for the given resonance. To change to other resonances it is necessary to know the relative variation of the flux with the energy and to estimate the change in the efficiency on going from resonance to resonance. The energy dependence of the flux was measured with boron counters. As to the efficiency with which radiation capture is registered, it should not vary noticeably from resonance to resonance, since the γ -ray spectrum is due to the large number of transitions to intermediate levels common to the resonances of one isotope. The presence of two isotopes of natural bromine can lead to some difference in the efficiency for resonances of different isotopes. In addition, the γ -ray spectrum may exhibit some dependence on the level spin.

To check the constancy of the neutron radiative-capture registration efficiency ϵ_γ in different resonances, additional measurements were made. The same detector was used to plot the amplitude spectra of the γ rays produced by neutron capture in resonances of Br^{79} and Br^{81} . The apparatus spectra coincided fully. Further, measurements were made in the summation mode in addition to the principal measurements in the coincidence mode. In the summation mode the efficiency for the registration of the (n, γ) reaction depends little on the form of the spectrum and on the multiplicity of the γ quanta per neutron capture. As shown by the measurement results, the ratio of the total number of counts did not vary from resonance to resonance in the different modes. This allows us to assume that the efficiency ϵ_γ is constant for all the resonances.

Using the values obtained for $\Pi(E)\epsilon_\gamma$, it was possible to obtain the experimental values of C for all the investigated resonances. These values were corrected for neutron capture in the sample following the scattering [8] and for the registration of the scattered neutrons by the detector. The latter correction was calculated from the formula

$$C = C_{\text{exp}}/(1 + \Gamma_n\epsilon_n/\Gamma_\gamma\epsilon_\gamma)$$

and was less than 2 per cent for all the investigated resonances. Equation (4) enables us to plot $g\Gamma_n$ against Γ for two possible values of the spin factor g .

In addition to the described experiment, it is possible to measure with the aid of the $n\gamma$ detector the resonance parameters by the self-indication method, described in detail by Rosen et al [9,10]. The gist of the method consists in carrying out, in addition to measurements of the type described above, also measurements with an additional sample T made of the same material, located outside the detector under "good geometry" conditions.

From the ratio of the total counting rates for a given resonance with and without the sample T we readily obtain the expression

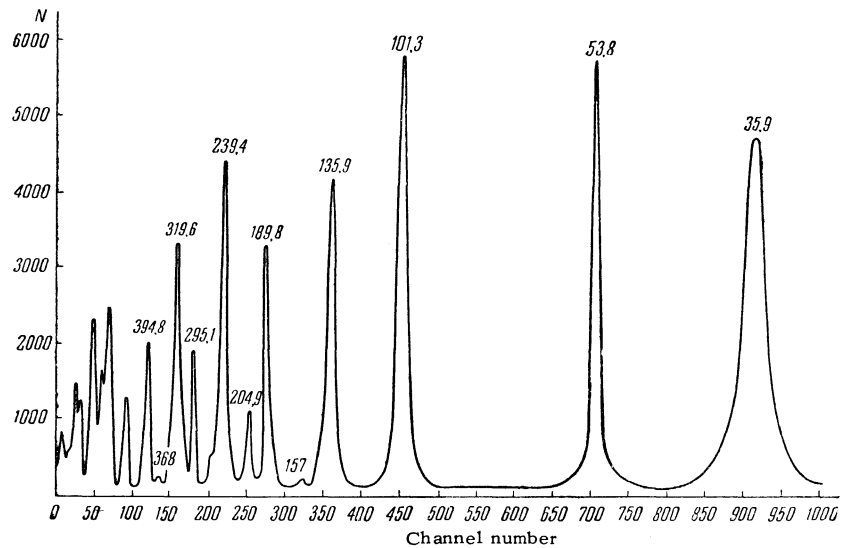
$$S = \frac{\Sigma N(D, T)}{\Sigma N(D)} \exp(n_T\sigma_p) = \frac{A_{D+T} - A_T}{A_D}, \quad (6)$$

which does not contain the values of the flux and the detector efficiency, and is a function of the parameters that determine the value of A , and also of the ratio n_T/n_D and the potential scattering cross section σ_p . A table of the values of S was calculated with an electronic computer for a wide range of parameters. By determining S experimentally, we could obtain, in accordance with (6), the dependence of $g\Gamma_n$ on Γ .

The material used in the measurements was KBr powder in thin-wall aluminum cassettes 190 mm in diameter (collimator diameter 180 mm). The thicknesses of the specimens employed, both D and T , varied over a wide range so as to obtain the best measurement conditions for the different resonances. Measurements with the D -specimens were made at four thicknesses, from 0.325×10^{21} to 7.7×10^{21} nuclei/cm² of natural bromine isotope mixture (50.56% Br^{79} and 49.44% Br^{81}). Five of the T -specimens were 0.325×10^{21} to 61.6×10^{21} nuclei/cm² thick. To prepare the thinnest specimen $D_1 = T_1$ (0.325×10^{21} nuclei/cm²), the KBr was mixed with CaF_2 powder to obtain a more uniform distribution over the specimen area.

Figure 1 shows an experimental curve obtained in 8-hour measurements with a specimen D of

FIG. 1. Experimental curve for neutron resonances of bromine, obtained with $n\gamma$ detector. The numbers indicate the resonance energies in eV.



thickness 7.7×10^{21} nuclei/cm². The background level was determined on the basis of measurements without the specimen and of measurements with graphite, which yields only scattered neutrons. The results obtained are in good agreement with the level of the sections of the curve of Fig. 1 that are far from resonance, with allowance for the effect of the resonance wings.

Measurements with graphite made it possible to estimate the neutron registration efficiency, which was found to be approximately 0.15 per cent and independent of the neutron energy and the investigated region.

The error in the determination of C in (4) was due above all to the error in the determination of the product $\Pi(E)\epsilon_\gamma$, which was estimated at 8 per cent. The error due to the statistics of the summary number of counts for a given resonance was smaller. For strong resonances it amounted to 1–2 per cent, and for the weakest ones it reached 5–6 per cent. A considerable contribution to the error for the weak resonances was made by the uncertainty in the background level and in the separation of the weak resonances from the nearby strong resonances. For the weakest resonances, for example at 212 or 256 eV, this error reached 15 per cent. For the strong resonances it was small. The final error in C was determined as the square root of the sum of the squares of the errors listed above.

In the measurements by the self-indication method the error connected with the flux and with the efficiency was eliminated, but the error connected with the statistics was increased, since S is determined by the ratio of the total counting rate over the resonance width without the absorbing specimen. The summary error in S was 1–3

per cent for specimens of optimal thickness in the case of strong resonances. For the weakest resonances the error in S is noticeably larger, and the use of the self-indication method is not advantageous.

NEUTRON SCATTERING

For the case of neutron scattering we can write an expression for the summary number of detector counts, analogous to (2):

$$\sum N = \Pi(E) \epsilon_n \int [1 - \exp(-n\sigma_t)] \frac{\sigma_n}{\sigma_t} dE = \Pi(E) \epsilon_n I. \quad (7)$$

For the analysis that follows it is convenient to introduce the difference

$$I - I_p = \int \left\{ [1 - \exp(-n\sigma_t)] \frac{\sigma_n}{\sigma_t} - [1 - \exp(-n\sigma_p)] \right\} dE, \quad (8)$$

where I_p describes the total number of counts in the same energy interval, under the condition that only potential scattering takes place and $\Pi(E)\epsilon_n = 1$. Since thin specimens are used in scattering experiments ($n\sigma_0 \lesssim 1$), it is possible to expand the integrand in (8) in a series and retain the first few terms. After integration and grouping of terms we obtain

$$I - I_p = \frac{\Gamma_n}{\Gamma} A - \frac{\pi}{8} \Gamma (n\sigma_{i0})^2 M - \frac{\pi}{4} (n\sigma_0 \Gamma) (n\sigma_p) L. \quad (9)$$

Here $\sigma_{i0} = \sigma_0 \cdot 2a/\lambda$ is the term due to the interference between the potential and resonant scattering; A is the area of the dip on the transmission curve; M and L are polynomials that depend on $n\sigma_0$ and on Γ_n/Γ .

Let us consider in greater detail the physical meaning of the expression obtained. If the integration limits include fully the isolated resonance

under consideration, the difference $I - I_p$, multiplied by $\Pi(E)\epsilon_n$, is the difference between the experimental sum of the number of counts over the resonance region and the sum of the number of counts produced in the same channels only by the potential scattering in the absence of resonance. The latter quantity is determined by interpolating the level of the potential scattering from a region far from resonance, or from calibration measurements with a scatterer that has no resonances such as lead.

For further use, it is convenient to transform (9) into

$$A\Gamma_n/\Gamma = (I - I_p)/(1 - \Omega_M - \Omega_L). \quad (10)$$

As shown earlier^[11], the quantities Ω_M and Ω_L can be reduced with some degree of approximation to the form

$$\Omega_M = n\sigma_p g, \quad (11)$$

$$\Omega_L = \frac{1}{2} n\sigma_p (\Gamma/\Gamma_n + 1). \quad (12)$$

Since $n\sigma_p \ll 1$, is usually possible to neglect Ω_M . Considerably more important is the quantity Ω_L which in the case $\Gamma_n \ll \Gamma$ can turn out to be comparable with unity and may even exceed it. In this case $I - I_p$ will be a negative quantity, i.e., the experimental curve lies below the interpolation level of the potential scattering. This is due to the fact that the resonant capture of the neutrons reduces greatly the number of neutrons that experience potential scattering.

Particular notice must be made of the fact that although the composition of the scattering specimen includes nuclei other than those of the investigated isotope this should be taken into account in (12) by replacing $n\sigma_p$ with $\sum_i (n\sigma_p)_i$, where the sum is taken over all the nuclei present. This does not pertain to (11), where it is possible to retain the value of $n\sigma_p$ for the given isotope.

In the subsequent analysis we used expression (10). To find $I - I_p$ it was necessary to know the product $\Pi(E)\epsilon_n$, which was determined by calibration measurements with lead as a sample. The interaction between the neutrons and the lead nuclei was due to the potential scattering, the cross section of which, 11.4 b, was independent of the neutron energy in the region under consideration.

In this case the number of counts per time-analyzer channel is

$$N_{Pb} = \Pi(E) \epsilon_n [1 - T_{Pb}] \Delta E, \quad T_{Pb} = \exp(-n\sigma_p)_{Pb}, \quad (13)$$

where ΔE has the same meaning as in (1). Hence

$$\Pi(E) \epsilon_n = N_{Pb} / (1 - T_{Pb}) \Delta E, \quad (14)$$

where N_{Pb} and ΔE are taken for the channel corresponding to the maximum of the resonance.

The experimental value of the number of counts over the resonance is influenced by the neutron capture which follows the scattering and reduces the number of detector counts. To eliminate the effect of multiple interactions, measurements were made with several specimen thicknesses and the quantity

$$B = \frac{I - I_p}{1 - \Omega_M - \Omega_L} \frac{g\Gamma_n}{A} \quad (15)$$

was extrapolated to zero thickness. The quantity A in (15) is a function of the parameters $g\Gamma_n$, F , and the specimen thickness n , but on going to the limit as $n \rightarrow 0$ the ratio $A/g\Gamma_n$ does not depend on the chosen parameters and is a known quantity. We substituted in (15) values of $g\Gamma_n$ and A known from previous results.

Thus, extrapolation yields

$$\lim_{n \rightarrow 0} B = g\Gamma_n^2/\Gamma. \quad (16)$$

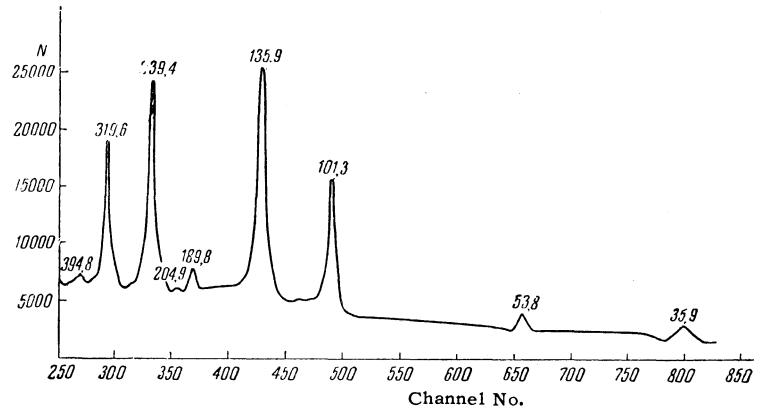
This equation gives the connection between $g\Gamma_n$ and Γ for two possible values of g and makes it possible, following simultaneous solution with Eqs. (4) and (6) to obtain all the parameters of the level.

Extrapolation not only eliminates the error connected with the capture after scattering, but has another beneficial effect. For thin specimens, the influence of the Doppler broadening on the area of the dip on the transmission curve becomes insignificant. The same holds for the analogous integral (8). Thus, extrapolation eliminates some inaccuracy connected with neglect of the Doppler broadening in the derivation of (10).

Neutron scattering was measured with specimens similar to those used with the γ detector, but in addition with thin specimens (0.16×10^{21} and 0.54×10^{21} nuclei/cm²) prepared by depositing KBr on thin substrates, so as to avoid the use of CaF₂, which increased the potential scattering. Figure 2 shows an experimental curve obtained with a specimen 4.14×10^{21} nuclei/cm² thick after 15 hours. The channel width is 8 μ sec.

In the calibration measurements we used four lead specimens 0.8 to 4 mm thick. In addition to the measurements with lead and bromine, the detector background was measured with the reactor in operation. The experimental error in the extrapolated value of B was determined principally by the statistics. To extrapolate B , a straight line was drawn by least squares through the weighted experimental points. The errors in the extrapolated value of B were 3–5% for strong resonances

FIG. 2. Experimental curve of neutron resonances of bromine, obtained with scattered-neutron detector (the numbers indicate the resonance energies in eV).



and reached 20% for the weakest resonances (204.9 and 394.8 eV), investigated with the aid of the scattered-neutron detector. The extrapolation plots for the two resonances are shown in Fig. 3.

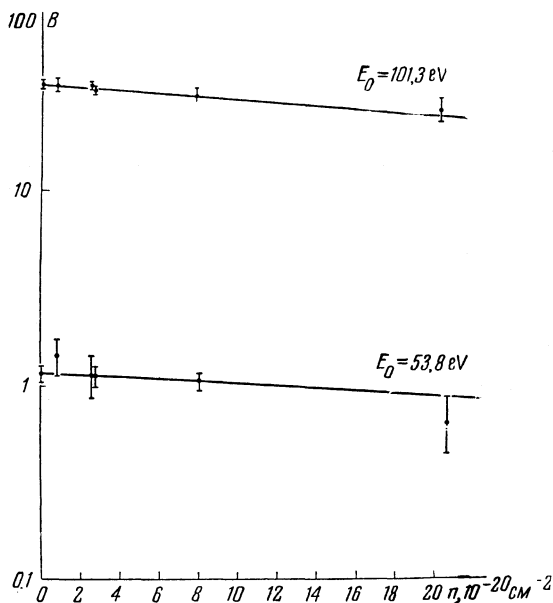


FIG. 3. Extrapolation plots of B (in MeV) for the 53.8 and 101.3 eV bromine resonances.

RESULTS AND DISCUSSION

The experimental data obtained in accordance with the procedure described above have made it possible to analyze the resonances lying at energies below 400 eV.

In addition to the ten resonances described in [1,2], five additional weak resonances were detected by the measurements with the $n\gamma$ detector. For these resonances it was possible only to make an estimate of $g\Gamma_n$, using formula (4). It was assumed that $\Gamma_\gamma/\Gamma = 1$. The total width for these resonances was not determined. For the remaining resonances the data reduction was in accordance with the complete program, except for the

resonance with energy 295.1 eV, for which the neutron-scattering data were not processed, owing to the insufficient resolution and statistics.

To obtain the parameters of the resonances, curves of $g\Gamma_n$ were plotted against Γ on the basis of (4), (6), and (16). Figures 4 and 5 show by way of an example the curves for two resonances with large and small neutron width. The curve S is a function of the parameters $g\Gamma_n$ and Γ , so that we have a single curve in these chosen coordinates. For the curves B and C there appears a third parameter, namely the spin factor g , which can assume two fixed values. For bromine, which has a spin $I = 3/2$, these values are $3/8$ and $5/8$. Thus, Eqs. (4) and (16) enable us to obtain different curves for different g . The true values of $g\Gamma_n$ and Γ for the given resonance should satisfy all three types of curves (S , B , and C). Since only one point of intersection of curves B and C lies on curve S , this indicates simultaneously the value of g , i.e., the level spin.

Figure 4 shows a family of curves for the resonance 101.3 eV. Curves C_1 , C_2 , and C_3 were obtained for different thicknesses of the detector specimen. It is seen that curve S agrees with curves B and C for $g = 5/8$. The curves for the

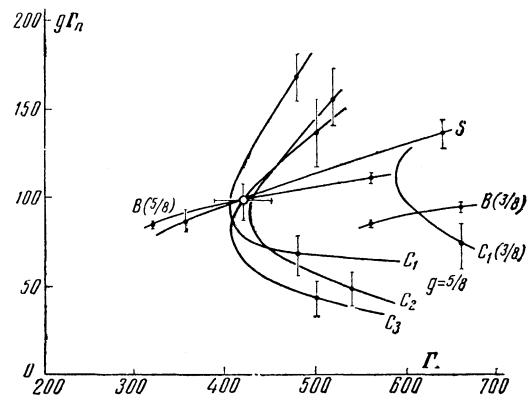


FIG. 4. 101.3-eV resonance. Family of curves plotted on the basis of Eqs. (4), (6), and (16); $g\Gamma_n$ and Γ are in MeV.

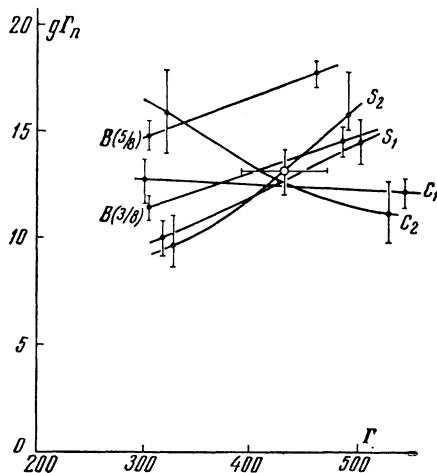


FIG. 5. 53.8-eV resonance. Family of curves plotted on the basis of Eqs. (4), (6), and (16); $g\Gamma_n$ and Γ are in MeV.

53.8-eV resonance, shown in Fig. 5, have a somewhat different character. The neutron width of this resonance is much smaller than the radiation width, so that $\Gamma_\gamma/\Gamma \approx 1$. In this case Eq. (4) goes over in practice into the relation $C \approx A$. This causes the curve C to become independent of g , and the only source of information on the spin remains curve B. It is seen from the figure that the point of intersection of the curves S and C lies on curve B for $g = 3/8$. Since for most bromine resonances the neutron widths are smaller than the radiation widths, the measurement of the neutron scattering was the principal method of determining the level spins.

It must be noted that the reliability of the S curve depends appreciably on the thicknesses of the chosen samples D and T, which have optimal values for each resonance. Since a large range of specimen thicknesses was used in the measurements, this has made it possible to choose those yielding the smallest uncertainty in the curve S.

The resonance parameters obtained by this method are listed in the table. The isotope identification is borrowed from [1]. A comparison of the parameters of the resonances given in [1,2] with the results of the present work shows agreement for most resonances, within the limits of the measurement errors. Level spins not hitherto published in the literature were obtained for nine bromine resonances.

The table was used to plot the distribution of the neutron widths. Since the isotope identification of the weak resonance is unknown, the distribution was plotted for all resonances.

The distribution obtained is shown in Fig. 6 together with the Porter-Thomas curve for the case $\nu = 1$. As can be seen from the figure, the experimental data do not contradict the theoretical curve, but the group of weak resonances deviates somewhat from the curve itself. It must be noted that in processing the experimental curves obtained with the $n\gamma$ detector there were hints of the presence of a few other levels, but the insufficient resolution did not make it possible to separate these weak levels for any degree of reliability, and these are therefore not listed in the table.

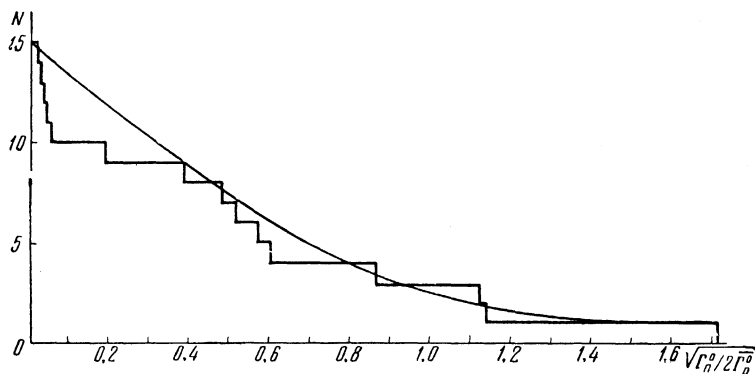
In this connection, it is of interest to carry out measurements with better resolution, so as to separate the weak resonances more reliably and to increase the number of analyzed levels, which so far is insufficient. The strength function $S_0 = \Gamma_n^0/D$ (where $\Gamma_n^0 = \Gamma_n/\sqrt{E}$) was calculated from the tabulated data with allowance for the spin levels for the Br^{79} isotope and found to be $(1.45 \pm 0.2) \times 10^{-4}$. For Br^{81} the strength function was not calculated because of the small number of resonances of this isotope.

The difference in the radiation widths for the isotopes Br^{81} ($\Gamma_\gamma = 275$ MeV) and Br^{79} ($\Gamma_\gamma = 400$ MeV) is striking. The neutron binding energies

Parameters of neutron resonances of bromine

E_0 , eV	Γ , meV	$g\Gamma_n$, meV	J	Γ_γ , meV	Isotope	Γ_n^0 , meV
35.9 ± 0.1	405 ± 30	25 ± 2	2	365 ± 30	79	6.7
53.8 ± 0.2	430 ± 40	13 ± 1	1	395 ± 40	79	4.7
101.3 ± 0.5	420 ± 30	97 ± 10	2	267 ± 33	81	15.4
135.9 ± 0.7	590 ± 50	115 ± 15	1	285 ± 52	81	26.5
157.3 ± 1.7	—	0.065 ± 0.015	—	—	—	—
189.8 ± 1.2	550 ± 60	28 ± 2	1	475 ± 60	79	5.4
204.9 ± 1.3	400 ± 60	6.5 ± 0.7	2	390 ± 60	—	0.73
212.4 ± 2.7	—	0.085 ± 0.02	—	—	—	—
239.4 ± 1.6	1300 ± 150	350 ± 50	1	365 ± 160	79	60.2
256 ± 3.6	—	0.135 ± 0.03	—	—	—	—
295.1 ± 2.2	460 ± 50	26 ± 2	—	408 ± 50	79	—
319.6 ± 2.5	800 ± 80	300 ± 40	2	320 ± 90	79	26.8
336 ± 5	—	0.41 ± 0.08	—	—	—	—
368 ± 6	—	0.26 ± 0.06	—	—	—	—
394.8 ± 3.5	610 ± 50	56 ± 6	1	460 ± 50	79	7.5

FIG. 6. Distribution of reduced neutron widths of bromine resonance. The smooth curve corresponds to the Porter-Thomas distribution with $\nu = 1$.



are practically the same for Br^{80} and Br^{82} . The ground-state spins of the target nuclei also are the same ($I = 3/2$), so that this cannot cause such a difference. The difference in the radiation widths is apparently connected with the appreciable difference in the spins of the ground state of the product nucleus, namely $I = 1$ for Br^{80} and $I = 5$ for Br^{82} .

No noticeable difference is observed in the neutron and radiation widths of the levels with different spins for the resonances of Br^{79} , for which the spins of six levels were determined.

In conclusion the authors consider it their pleasant duty to thank F. L. Shapiro for useful discussions and interest in the work, and I. I. Shelontsev and N. Yu. Shirikov for calculations on the electronic computer.

¹ Leblanc, Cote, and Bollinger, *Nucl. Phys.* **14**, 120 (1959).

² Rosen, Desjardins, Havens, and Rainwater, *Bull. Am. Phys. Soc.* **11**, 4, 473 (1959).

³ Blokhin, Blokhintsev, Blyumkina, et al., *Atomnaya énergiya* **10**, 437 (1961).

⁴ Matalin, Shimanskiï, Chubarov, and Shtranikh, *PTÉ* No. 3, 54 (1960).

⁵ Pikel'ner, Pshitula, Kim, Cheng, and Sharapov, *PTÉ* No. 2, 51 (1963).

⁶ Pikel'ner, Pshitula, Kim, Cheng, and Sharapov, *PTÉ* No. 2, 51 (1963).

⁷ V. N. Efimov and I. I. Shelontsev, Preprint, Joint Inst. Nuc. Res. R-641 (1961).

⁸ J. E. Draper, *Nucl. Sci. and Eng.* **1**, 522 (1956).

⁹ Rosen, Desjardins, Rainwater, and Havens, *Phys. Rev.* **118**, 687 (1960).

¹⁰ Desjardins, Rosen, Havens, and Rainwater, *Phys. Rev.* **120**, 2214 (1960).

¹¹ Zeliger, Iliescu, Kim, Longo, Pikel'ner, and Sharapov, Preprint Joint Inst. Nuc. Res. R-1218, Dubna, 1963.